Gold Bull (2012) 45:83–90
DOI 10.1007/s13404-012-0051-z

ORIGINAL PAPER

Formation of nanometer-sized Au particles on USY zeolites under hydrogen atmosphere

Kazu Okumura · Chika Murakami · Tetsuya Oyama · Takashi Sanada · Ayano Isoda · Naonobu Katada

Published online: 15 May 2012

Abstract Gold was deposited on ultrastable Y (USY) zeolite using a newly developed method: just mixing an aqueous solution of $HAuCl_4$ and zeolite at 353 K in which the NH_4^+ cation reacted with the Cl^- in $HAuCl_4$. Treatment of the Au-loaded USY zeolite in the atmosphere of hydrogen resulted in the formation of Au^0 nanoclusters with 1.8 nm diameter at 773 K. The size of Au particle was dependent on the type of zeolite support, composition of gas atmosphere, and temperature of calcination, which was correlated with catalytic performance. This study demonstrated the potential use of zeolites with strong Brønsted acid character as gold supports.

Keywords Gold cluster · Nanoparticle · USY zeolite · Brønsted acid · Homocoupling

Introduction

Since the pioneering work by Haruta and co-researchers, efforts have increasingly been directed toward the development of supported Au catalysts [1–4]. Interest in these catalysts is fuelled by their unique catalytic performance in various reactions [5, 6]. The catalytic performance of Au particles is sensitive to the Au particle size, and consequently, the regulation of the size of Au particles is of fundamental importance for the application to catalytic reactions [7]. In particular, high catalytic performance has been reported for Au particles smaller than several nanometers in size [1]. Preceding reports primarily focused on the use of reducible metal oxides such as TiO_2 and Fe_2O_3 as supports for Au. Other researchers attempted to use zeolites as the supports for Au. For instance, Au loaded on Y-type zeolites has been applied to CO oxidation [8]. Reduction of NO by H_2 has been performed over Au^0 or Au(I) loaded on Na^+–Y zeolite [9], and the formation of electron-deficient gold particles inside H–Y cavities has been observed [10]. Propene epoxidation by H_2 and O_2 was carried out over Au/TS-1 [11]. We have also utilized H–Y zeolites as a support for Au [12, 13]. Zeolites are promising supports for metals because the presence of strongly acidic sites in these materials promotes high dispersion of metal particles. In fact, metal clusters of Pd and Pt with high dispersion were obtained on zeolites having Brønsted acid sites [14, 15]. Ultrastable Y (USY) zeolites contain strongly acid sites [16] (ca. 150 kJ mol^{-1}) and also exhibit high thermal stability. These acidic sites may be exploited for interaction with Au, and their thermal stability makes USY zeolites attractive for use as Au catalyst supports in high-temperature applications.

To date, several methods including precipitation deposition [17], chemical vapor deposition [18], and cation adsorption [19] have been applied for the preparation of Au/TiO_2 catalysts. Cation exchange using $[Au(en)_2]^{3+}$ and incipient wetness impregnation have been employed for the loading of zeolites [20, 21].

The purpose of this study is to establish a new method for the preparation of Au nanoclusters on zeolite supports, demonstrating that nanometer-sized Au^0 particles having a narrow size distribution were obtained after calcination at

K. Okumura (✉) · C. Murakami · T. Oyama · T. Sanada · N. Katada
Department of Chemistry and Biotechnology,
Graduate School of Engineering, Tottori University,
4-101 Koyama-cho Minami,
Tottori 680-8552, Japan
e-mail: okmr@chem.tottori-u.ac.jp

T. Sanada · A. Isoda
Research Department, NISSAN ARC, LTD.,
Yokosuka 237-0061, Japan

temperature higher than 573 K. Moreover, the influences of the concentration of hydrogen in the gas phase and the Brønsted acid strength on the size of Au particles were investigated. Preliminary data were recently reported elsewhere as a communication [22]. In the present study, USY zeolite is used as a support for Au. First, we developed a new method for loading Au on the zeolite support in which Au was loaded on NH_4^+-type USY zeolites using an aqueous solution of $HAuCl_4$. Then, the as-prepared Au/USY was thermally treated in an atmosphere of H_2 from 353 to 773 K. Changes in the local structure and size of Au were analyzed by X-ray absorption fine structure (XAFS), X-ray diffraction (XRD), and transmission electron microscopy (TEM). Homocoupling of phenylboronic acid was performed as the catalytic reaction. The reason of the choice of this reaction was that the acid sites present in zeolites were supposed not to be influential on the homocoupling reaction.

Experimental

Sample preparation

Gold was loaded on an NH_4-type USY zeolite (Tosoh, HSZ-341NHA, $Si/Al_2=7.7$) using $HAuCl_4{\cdot}4H_2O$ (Wako Chemical Co.) as the precursor. The USY (1 g) was immersed in an aqueous solution of $HAuCl_4$ (250 mL, 6.1×10^{-4} mol L^{-1}), and the slurry was kept at 343 K for 1 h with constant stirring. The Au-loaded USY zeolite was filtered, washed with deionized water, and dried in an oven at 323 K. The loading of Au was most commonly 3 wt% as measured by inductively coupled plasma. The obtained Au/USY was typically treated with a stream of 6 % H_2 diluted with Ar at a given temperature for 30 min. Temperature ramping rate for the treatment was 5 K min^{-1}. Au/USY samples are henceforth denoted as Au/USY-x in which x represented the calcination temperature. Loading of Au on $CaNH_4^+$-type Y and NH_4^+-type Y, NH_4NO_3-treated USY was carried out in a similar way as described for the preparation of Au/USY. Concentration of Ca in CaH–Y was 1.0 mol kg^{-1}. Precipitation–deposition method was employed for the loading of 3 wt% Au on H-ZSM-5 (JRC-Z5-90H(1),$Si/Al_2=90$), H-mordenite (JRC-Z-HM15, $Si/Al_2=15$), and TiO_2 (JRC-TIO-11), which were supplied by the Catalysis Society of Japan.

TEM, XAFS, and XRD data collection and analysis

TEM images were acquired using a HITACHI H-9000UHR microscope with an acceleration voltage of 300 kV. Synchrotron radiation experiments (XAFS) were performed at the BL01B1 station with the approval of the Japan Synchrotron Radiation Research Institute (Proposal No. 2011A1106, 2011B1095). A Si(111) single crystal was used to obtain a monochromatic X-ray beam. Measurements were recorded in the quick mode at room temperature. For the collection of Au L_3-edge data, ion chambers filled with N_2 and a mixture of N_2 (50 %)/Ar (50 %) were used for I_0 and I, respectively. The energy was calibrated using an Au foil. The data were analyzed using the REX2000 Ver. 2.5.9 program (Rigaku Co.). Fourier transform of $k^3\chi(k)$ data was performed in a k range 30–160 nm^{-1} for the analysis of the Au L_3-edge extended X-ray absorption fine structure (EXAFS) spectra. The inversely Fourier filtered data were analyzed using a common curve-fitting method. The empirical phase shift and amplitude functions for Au–O and Au–Au were extracted from the data of FEFF code (ver. 8) and Au foil, respectively. The crystalline structure was analyzed by XRD under ambient conditions using a Rigaku Ultima IV X-ray diffractometer with Cu Kα radiation.

Catalytic reactions

The samples were pretreated in 6 % H_2 at a given temperature before being used in homocoupling reaction of phenylboronic acid. The treated samples were stored in the dark prior to the reaction. Homocoupling reactions were carried out over the Au catalysts. Phenylboronic acid (0.25 mmol; Tokyo Kasei Chemicals Ltd., Japan), K_2CO_3 (0.75 mmol; Wako Chemicals Ltd., Osaka, Japan), deionized water (solvent, 5 mL), and Au-loaded catalyst (16.4 mg) were used for the reaction. Molar amount of gold was 1 mol% with respect to phenylboronic acid. A sample bottle (20 mL) was placed on a magnetic stirrer and subjected to vigorous stirring. The reaction was performed at 300 K under atmospheric conditions for 0.5 h. The reaction was quenched by the addition of ethyl acetate. The product was extracted with ethyl acetate. Following evaporation of the ethyl acetate, the residue was analyzed by gas chromatography [Shimadzu 2010 Gas Chromatograph equipped with an InertCap 1 (30 m) capillary column (Shimadzu Corp., Kyoto, Japan)]. Tridecane was used as the internal standard.

Results and discussion

Influence of the calcination temperature on Au dispersion

In the preparation of Au/USY, Au was loaded on NH_4–USY using $HAuCl_4$ as the Au precursor. The solution of $HAuCl_4$ had been yellow and it was decolorized, while the zeolites became a pale orange color within 1 h after temperature of the solution reached 343 K. These changes in color indicate the loading of Au on USY. Formation of NH_4Cl in the filtered solution was confirmed by means of IR, XRD, and TG analysis. The molar amount of NH_4Cl dissolved in the

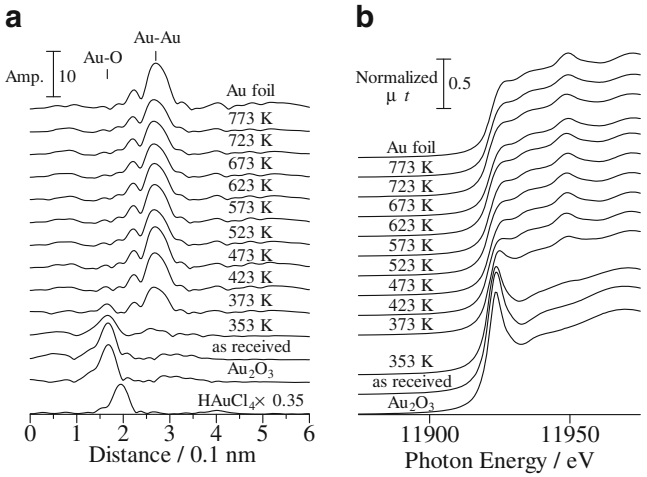

Fig. 1 Au-L_3 edge EXAFS $k^3\chi(k)$ Fourier transforms (**a**) and XANES (**b**) of 3 wt% Au/USY treated at different temperatures under 6 % H_2 atmosphere and reference samples. Data collection was carried out at room temperature

solution was four times larger than that of Au, suggesting the following stoichiometry (Eq. 1).

$$AuCl_4^- + 4NH_4^+ - \text{zeolite} \rightarrow Au^{3+} - \text{zeolite} + 4NH_4Cl \quad (1)$$

The Au^{3+} zeolite was hydrated by water to give Au_2O_3 simultaneously according to Eq. 2:

$$2Au^{3+} - \text{zeolite} + 3H_2O \rightarrow Au_2O_3 + 6H^+ - \text{zeolite} \quad (2)$$

The ion exchange sites of USY zeolite should be partially exchanged with H^+. Formation of Au_2O_3 in the as-prepared sample was confirmed by EXAFS, as mentioned later. Deposition of Au also proceeded smoothly on NH_4–Y as confirmed by ICP analysis. In addition, Au was readily supported on NH_4^+-type USY even at higher loadings of 5 wt%. In marked contrast to the NH_4^+-type USY, Au was not deposited on either H^+-type USY or Na^+-type Y in a same method; this indicated that the presence of NH_4^+ cation is indispensable for the loading of Au. Loading of Au on NH_4^+-type ZSM5 and mordenite by a same procedure was also attempted. However, deposition of Au was not successful on other kinds of zeolites, except for Y-type materials. Therefore, deposition of Au specifically took place on the NH_4^+-type Y and USY zeolites.

Figure 1a shows Au-L_3 edge EXAFS of 3 wt% Au/USY. The Fourier transform of the as-received sample was identical to those of Au_2O_3. The Au–O bond appears at 0.17 nm (phase shift uncorrected). The features of spectrum in the range 0.25–0.40 nm were also similar to those of Au_2O_3. The peak corresponding to the Au–Cl was not observed in the Fourier transform. The absence of Au–Cl can be confirmed by comparison with $HAuCl_4$ in which the Au–Cl bond appears at ca. 0.20 nm (phase shift uncorrected), indicating that Au was successfully loaded on USY as aggregated Au_2O_3. The Au–O peak was decreased by H_2 treatment with temperature elevation, and the peak disappeared at 473 K. Alternatively, a new peak appeared at 0.27 nm, which was assignable to the nearest neighbor Au–Au bond in Au^0 metal on the basis of comparison with the spectrum of Au foil. The complete disappearance of the Au–O peak at 473 K indicates the formation of Au^0 as a result of H_2 reduction at this temperature. Formation of Au^0 at 473 K was also confirmed from the X-ray absorption near edge structure (XANES) regions; the shapes of the XANES profiles were markedly similar to that of Au foil, as shown in Fig. 1b. At temperatures above 473 K, the intensity of EXAFS peak corresponding to the Au–Au bond decreased slightly (Fig. 1a). This slight change suggests a decrease in the size of Au particles. The coordination numbers (CNs) of the nearest neighboring Au–Au bond in Au/USY samples treated at 473 and 773 K were calculated to be 11.8±1.6 and 9.6±1.4, respectively. The change in CNs of Au–Au atoms suggested the decrease in the size of the Au particles at higher treatment temperatures. The particle size of the Au/USY-773 K was estimated to be 2 nm on the basis of the CN=9.6, assuming a cuboctahedron shape [23].

Because EXAFS analysis is rather insensitive to CNs when the particle size of a metal is larger than several nanometers, Au/USY was analyzed by XRD, which is sensitive to changes in size of Au particles larger than several nanometers. Figure 2 shows the XRD patterns of the 3 and 5 wt% Au/USY samples treated at various temperatures. The peaks at 2θ=38.2° and 44.4° were due to the diffractions from the (111) and (200) planes of Au^0, respectively. Weak diffractions due to the USY zeolites appeared at 38.1° and 44.2°, which overlapped with the diffractions from Au^0. The intensity of the reflections from the Au^0(111) and (200) planes increased with increasing the treatment temperature from room temperature to 473 K on the 3 wt% H_2-treated

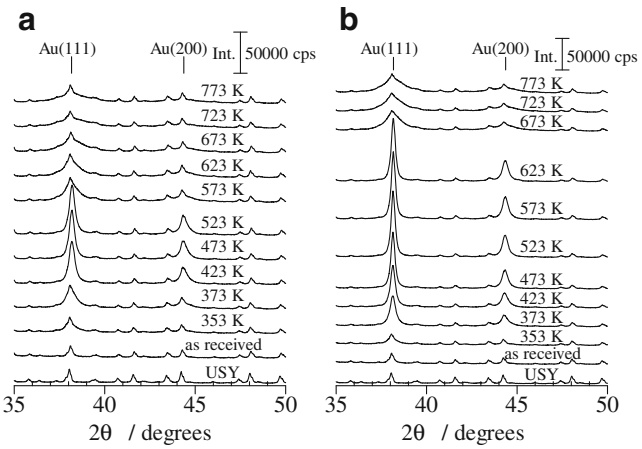

Fig. 2 XRD patterns of Au/USY treated at different temperatures under a 6 % H_2 atmosphere: **a** 3 wt% and **b** 5 wt%

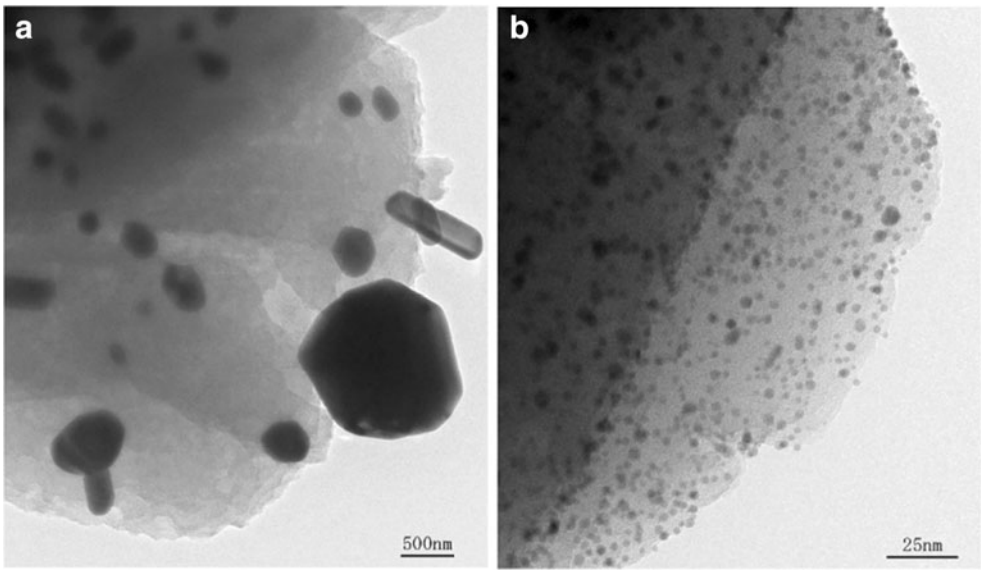

Fig. 3 TEM images of Au/USY calcined at **a** 473 K and **b** 773 K under an atmosphere of 6 % H_2. Loading of Au was 3 wt%

samples (Fig. 2a). This change can be attributed to the formation of Au^0 as confirmed by Au-L_3 edge XAFS (EXAFS and XANES). On further increase of the temperature, the intensity of these diffractions decreases, accompanied by peak broadening. A marked reduction of the peaks can be observed at 573 K indicating that highly dispersed Au particles were obtained when the treatment temperature was increased from 473 to 773 K. The XRD patterns of 5 wt% Au-loaded USY (Fig. 2b) exhibit a similar reduction of the Au(111) and Au(200) peaks indicative of dispersion of the Au^0 particles. However, the reduction in peak intensity was observed in the 5 wt% sample at 673 K, which was 100 K higher in the temperature than that for 3 wt% Au/USY, suggesting that the extent of Au loading impacts the behavior of Au.

TEM analysis was employed to directly observe the Au^0 particles on Au/USY in order to confirm the dispersion of Au. The TEM images of Au/USY treated at 473 and 773 K under a 6 % H_2 atmosphere are shown in Fig. 3a, b, respectively. Large Au^0 particles with a variation of size were observed in the image of Au/USY treated at 473 K (Fig. 3a). The shape of the Au particles was not uniform. In marked contrast to this, and in agreement with the EXAFS and XRD, the particles of Au^0 in Au/USY-773 K (Fig. 3b) were much smaller and seem to have a homogeneous size distribution compared to the sample treated at 473 K. Figure 4 shows the particle size distribution of Au^0 determined from the TEM images. The Au^0 particle sizes ranged from 10 to 150 nm with an average size of 25 nm for Au/USY-473 K. The average size of Au^0 in Au/USY-773 K was 1.8 nm, 1/14 of that of Au/USY-473 K. The estimated size is consistent with the Au L_3-edge EXAFS analysis. The mean diameter of Au (1.8 nm) is slightly larger than the diameter of super cages of in Y-type zeolite (1.3 nm), suggesting that most of the loaded Au was located on the external surface of zeolite. The distribution of Au^0 particle size in Au/USY-773 K ranges from 0.4 and 5.9 nm, significantly narrower as compared to that in Au/USY-473 K.

The formation of highly dispersed Au^0 at 773 K thus demonstrated by TEM coupled with EXAFS and XRD is unusual, because supported metal particles generally undergo sintering to form aggregates at high temperature in reductive atmosphere. It has been known that oxidative atmosphere can keep small particles of metal oxides; dispersion of Pd and Pt as cations has been observed under an atmosphere of oxygen [24]. We have also reported the spontaneous dispersion of molecular-like PdO on H-ZSM-5 [25]. In contrast to the above-mentioned examples, the dispersed Au^0 was obtained on USY zeolite support under an atmosphere of H_2 at high temperature in the present study. The origin of dispersion of Au^0 on USY zeolites has not been fully elucidated on this stage; however, one hypothesis is that the interaction of Au and H^+ generated as a result of thermal decomposition of NH_4^+ causes the dispersion of Au on the external surface of USY zeolites. As a matter of fact, Sachtler et al. proposed the possibility of the generation of $[Pd_n\ H]^+$ adducts encaged in zeolite pores [26,

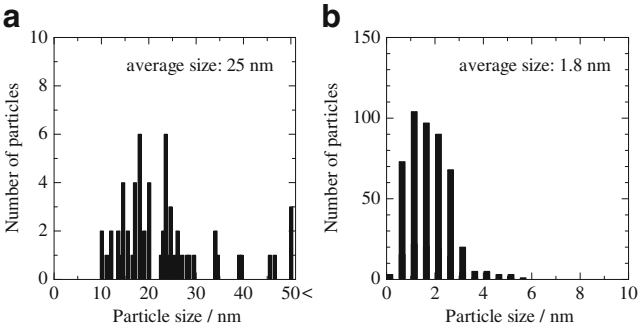

Fig. 4 Distribution of Au/USY calcined at **a** 473 K and **b** 773 K under an atmosphere of 6 % H_2. Loading of Au was 3 wt%

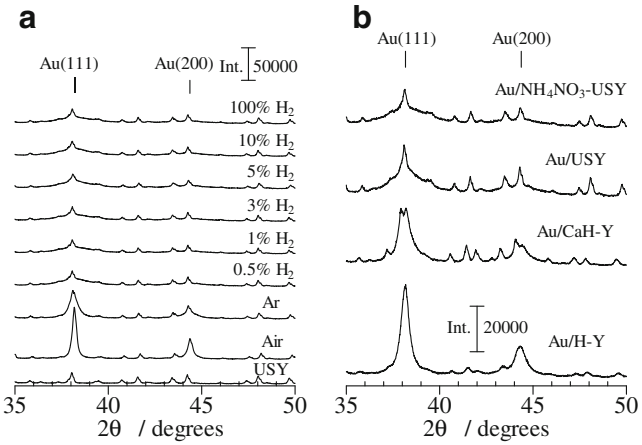

Fig. 5 XRD patterns of **a** Au/USY treated at 773 K in different atmosphere for 0.5 h, **b** Au loaded on Y-type zeolites calcined at 773 K in 6 % H_2

27]. Similarly, Fraissard et al. reported the chemical anchoring of Au clusters by the Brønsted sites of the support in Au/Y-type zeolites [20].

Influence of the concentration of H_2 and time on the dispersion of Au

Figure 5a shows XRD patterns of 3 wt% Au/USY treated under different atmospheres at 773 K. Steep diffraction peaks appeared in the samples calcined in air or Ar, namely 0 % H_2. Addition of 0.5 % H_2 to the atmosphere resulted in the formation of dispersed Au as confirmed from the broadening of diffraction peaks due to metal Au. No further change was observed with increasing the hydrogen concentration up to 100 %, leading us to conclude that the presence of low levels of hydrogen is sufficient to give rise to the dispersion to give nanometer-sized Au clusters. Figure 6 shows TEM images and particle size distribution of 3 wt% Au/USY treated under an atmosphere containing Ar and 0.5 % H_2, corresponding to the samples in Fig. 5a, respectively. The sizes of Au particles in the sample treated in the atmosphere of Ar are distributed over 4 to 59 nm with an average diameter of 14.6 nm. In marked contrast to Au/USY treated in Ar, the distribution (1–8 nm) of the size of Au treated under an atmosphere of 0.5 % H_2 is narrower and the average size (3.7 nm) is appreciably smaller. The treatment times of Au/USY were varied from 10 min to 10 h under an atmosphere comprising 6 % H_2 at 773 K. No differences were observed in the diffraction patterns obtained for these samples, implying that dispersion of Au occurs immediately when the temperature reaches 773 K. Although the role of hydrogen is not clearly understood at this stage, the TEM images of Au/USY treated in different atmospheres indicate that the presence of hydrogen has a profound influence on the dispersion of Au.

Influence of the acid strength of supports on the dispersion of Au

The acid strength of Brønsted acid sites present in Y-type zeolites can be finely tuned by (a) the introduction of divalent cations such as Ca^{2+} and (b) by dealumination in combination with posttreatment employing an aqueous solution of ammonium salts [16]. The influence of the acid strength on the dispersion of Au was examined by employing four types of Y-type zeolite supports: H–Y, CaH–Y, USY, and NH_4NO_3-treated USY. The highest acid strengths (heat of ammonia desorption) of the Brønsted acid sites present in H–Y, CaH–Y, USY, and NH_4NO_3-treated USY are 109, 122, 140, and 157 kJ mol^{-1}, respectively. The acid strength increased in the following order: H–Y<CaH–Y<USY<NH_4NO_3-treated USY. In the preparation of CaH–Y support, 30 % of NH_4^+ present in NH_4^+-type Y was exchanged with Ca^{2+} using $Ca(NO_3)_2$. Figure 5b shows XRD patterns of 3 wt% Au loaded on these supports. The samples were calcined at 773 K under a 6 % H_2 atmosphere. It can be seen that the intensity of the diffractions assignable to the Au(111) and (200) decrease with an increase in the intensity of acid strength of Y-type supports, suggesting that the greater the acid strength, the smaller the Au particles become.

Figure 7 displays TEM images of Au loaded on different Y-type zeolites, corresponding to the XRD patterns of

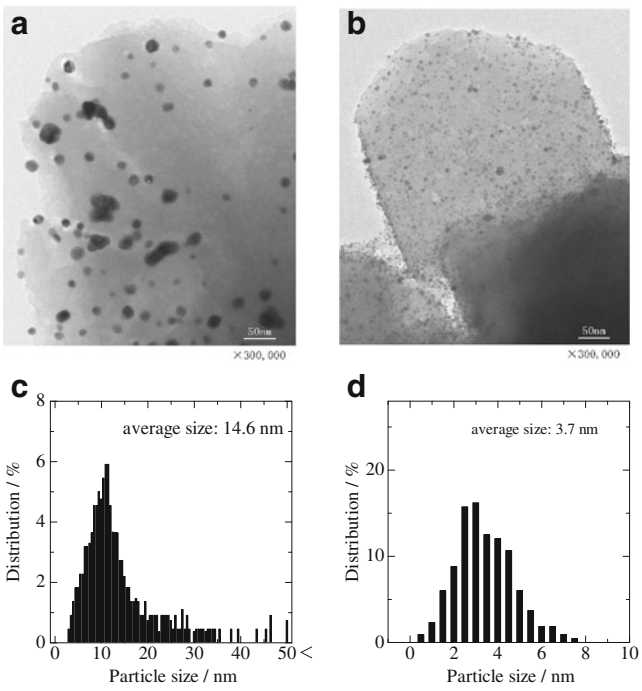

Fig. 6 TEM images of Au/USY calcined in **a** Ar and **b** 0.5 % H_2 at 773 K. Distribution of Au particles in 3 wt% Au loaded on USY calcined in (**c**) Ar and (**d**) 0.5 % H_2

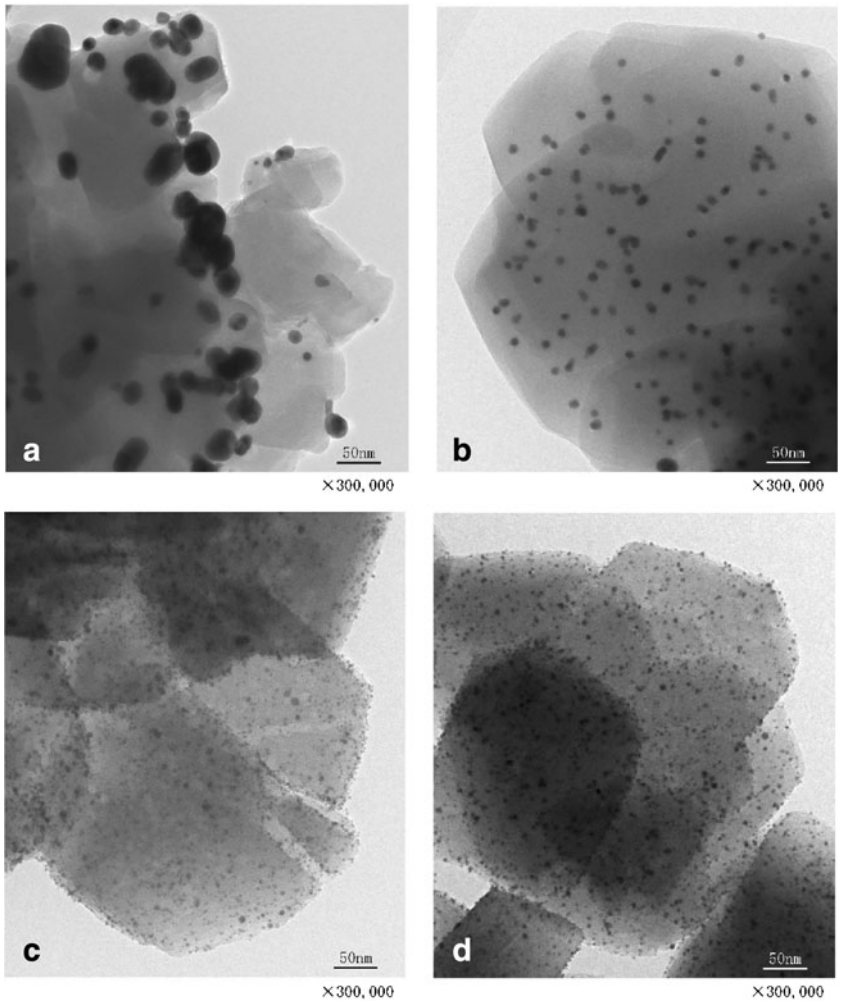

Fig. 7 TEM images of 3 wt% Au loaded on **a** H–Y, **b** CaH–Y, **c** USY, and **d** NH_4NO_3–USY

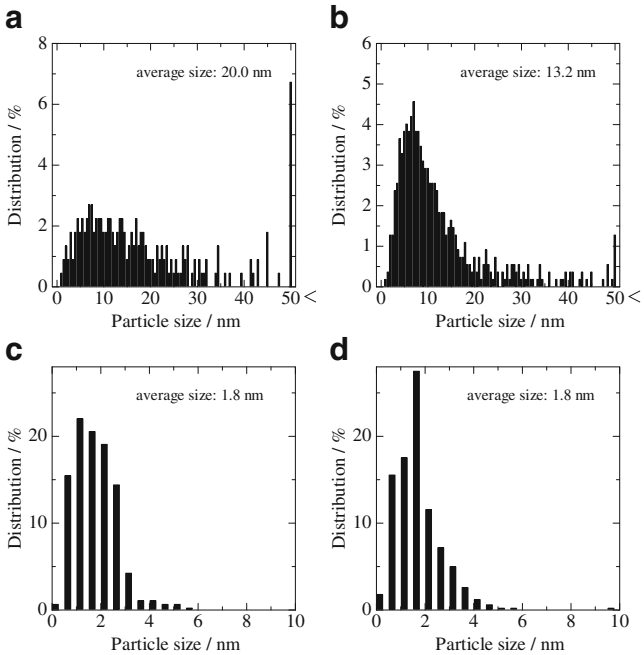

Fig. 8 Distribution of Au particles in 3 wt% Au loaded on **a** H–Y, **b** CaH–Y, **c** USY, and **d** NH_4NO_3–USY

Fig. 5b. The distribution of the size of Au particles in these samples is summarized in Fig. 8. An inhomogeneous distribution of large Au particles can be seen in the image of Au/H–Y (Fig. 7a). The size distribution plot confirms this observation (Fig. 8a). In the case of Au/CaH–Y, uniform Au particles ca. 10 nm in diameter can

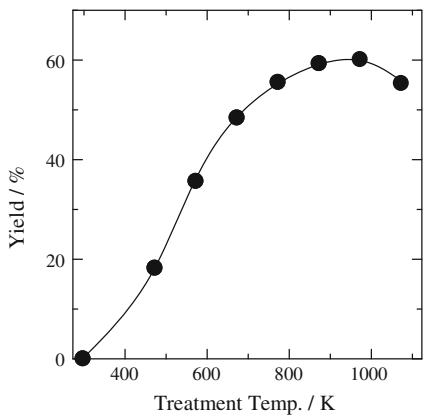

Fig. 9 Dependence of the yield of product (biphenyl) on the calcination temperature of 3 wt% Au/USY treated in a stream of 6 % H_2

be seen (Fig. 7b). Although the size distribution of Au particles in Au/CaH–Y is much narrower compared to that of Au/H–Y, some large particles can also be observed in the TEM images. The average particle size of Au loaded on USY and NH_4NO_3-treated USY is 1.8 nm, a significantly smaller value than those of Au particles loaded on H–Y and CaH–Y. Despite the identical average size of Au in the USY and NH_4NO_3–USY (1.8 nm), the Au/NH_4NO_3–USY shows a narrower distribution compared to Au/USY. The TEM images in combination with XRD patterns prove that the size of the Au particles is dependent on the acid strength of Y-type zeolites, indicating that the presence of the strong Brønsted acid sites induces the formation of nanometer-sized Au particles with a narrow size distribution.

Catalytic performance in the homocoupling reaction

The homocoupling reaction of phenylboronic acid was carried out over the Au-loaded catalysts. Figure 9 shows the yield of biphenyl product plotted as a function of calcination temperature of 3 wt% Au/USY. The yield of biphenyl increased as the calcination temperature increased. The highest yield (60 %) was obtained when the catalyst was calcined at 773–1,073 K. The catalytic activity of the Au/USY was equal to the performance of Au nanoclusters protected by PVP polymers [28]. The change in the particle size of Au can be seen to influence the catalytic activity; the yield of biphenyl increases as the particle size of Au particles decreases. Formation of biphenyl was negligible over USY zeolites without the loading of Au.

Catalytic reaction was carried out over 1.8-nm-sized Au-loaded USY in which the acid sites were changed to NH_4^+ through the exposure of NH_3. The yield of biphenyl over the Au loaded on NH_4^+-type USY (60 %) was close to that obtained in Au loaded on H^+-type USY, meaning the acid sites were not influential on the catalytic performance of Au.

Au was loaded on different types of support using the deposition precipitation method. The yields of biphenyl obtained with Au/TiO_2, ZSM-5, mordenite, and Na–Y were 35, 35, 36, and 4 %, respectively. The yields obtained with Au/H–Y and CaH–Y were and 16 and 17 %, respectively, lower than that obtained with Au/USY-773-1,073 K; this indicated that Au loaded on the USY zeolite afforded the highest activity. Calcination atmosphere affected the catalytic activity significantly as expected from the difference in the dispersion. The yields of biphenyl obtained with Au/USY calcined in Ar and air were 18 and 6 % respectively, which was much lower than that obtained after calcination in the atmosphere of H_2 (60 %).

Conclusions

Reduction of Au_2O_3 on USY zeolites exhibiting strong Brønsted acid character, in the presence of hydrogen, afforded nanometer-sized Au clusters with mean diameter of 1.8 nm. Various factors including temperature (>573 K), composition of gas phase (hydrogen), and acid strength (USY zeolites exhibiting strong Brønsted acid) of the support were shown to greatly influence the dispersion of Au. For instance, the average size of Au particles in Au/USY (1.8 nm) was 11 times smaller than that of Au/H–Y (20 nm). The catalytic activity of Au/USY in the homocoupling reaction of phenylboronic acid was in good correlation with the dispersion of Au. That is to say, the yield of biphenyl increased from 16 % (Au/H–Y) to 60 % (Au/USY) by employing the USY supports having strong acid character ca. 150 kJ mol^{-1}. The simplicity of technique used for loading of Au should be emphasized; stirring a solution of $HAuCl_4$ and NH_4^+-type USY zeolite at 343 K afforded Au_2O_3. This study shows the possibility of regulating the size of metal particles by making use of the strong interactions between Au and zeolite supports.

References

1. Haruta M (1997) Catal Today 36:153
2. Daniel MC, Astruc D (2004) Chem Rev 104:293
3. Haruta M (2004) Gold Bulletin 37:27
4. Bond GC, Thompson DT (1999) Catal Rev 41:319
5. Haruta M, Date M (2001) Appl Catal A 222:427
6. Corma A, Garcia H (2096) Chem Soc Rev 2008:37
7. Subramanian V, Wolf EE, Kamat PV (2004) J Am Chem Soc 126:4943
8. Fierro-Gonzalez JC, Gates BC (2004) J Phys Chem B 108:16999
9. Salama TM, Ohnishi R, Shido T, Ichikawa M (1996) J Catal 162:169
10. Guillemot D, Borovkov VY, Kazansky VB, PolissetThfoin M, Fraissard J (1997) J Chem Soc Faraday Trans 93:3587
11. Huang JH, Lima E, Akita T, Guzman A, Qi CX, Takei T, Haruta M (2011) J Catal 278:8
12. Okumura K, Yoshino K, Kato K, Niwa M (2005) J Phys Chem B 109:12380
13. Shimizu K, Yamamoto T, Tai Y, Okumura K, Satsuma A (2011) Appl Catal A 400:171
14. Okumura K, Yoshimoto R, Uruga T, Tanida H, Kato K, Yokota S, Niwa M (2004) J Phys Chem B 108:6250
15. Treesukol P, Srisuk K, Limtrakul J, Truong TN (2005) J Phys Chem B 109:11940

16. Okumura K, Tomiyama T, Morishita N, Sanada T, Kamiguchi K, Katada N, Niwa M (2011) Appl Catal A 405:8
17. Hayashi T, Tanaka K, Haruta M (1998) J Catal 178:566
18. Okumura M, Nakamura S, Tsubota S, Nakamura T, Azuma M, Haruta M (1998) Catal Lett 51:53
19. Zanella R, Giorgio S, Henry CR, Louis C (2002) J Phys Chem B 106:7634
20. Riahi G, Guillemot D, Polisset-Thfoin M, Khodadadi AA, Fraissard J (2002) Catal Today 72:115
21. Delannoy L, El Hassan N, Musi A, Le To NN, Krafft JM, Louis C (2006) J Phys Chem B 110:22471
22. Sanada T, Okumura K, Murakami C, Oyama T, Isoda A, Katada N (2012) Chem Lett 41:337
23. Jentys A (1999) PhysChemChemPhys 1:4059
24. Bera P, Patil KC, Jayaram V, Subbanna GN, Hegde MS (2000) J Catal 196:293
25. Okumura K, Amano J, Yasunobu N, Niwa M (2000) J Phys Chem B 104:1050
26. Homeyer ST, Karpinski Z, Sachtler WMH (1990) J Catal 123:60
27. Bai XL, Sachtler WMH (1991) J Catal 129:121
28. Tsunoyama H, Sakurai H, Ichikuni N, Negishi Y, Tsukuda T (2004) Langmuir 20:11293